
# Interaction of Barchan Dunes with Obstacles

## Under the guidance of Prof. Rajesh Ganapathy at JNCASR, Bengaluru

2024-07-31

**Diptanuj Sarkar**
Indian Institute of Science Education and Research, Kolkata
2024

# List of contents

# I. Introduction

Barchan dunes, characterized by their crescent-shaped morphology and unidirectional movement, are a common feature in arid and semi-arid regions. These dunes are formed by the action of wind on loose, dry sand and are typically oriented with their convex side facing upwind. Understanding the behavior of barchan dunes is crucial for a variety of scientific and practical reasons, including the study of desertification processes, the planning of infrastructure in desert areas, and the interpretation of extraterrestrial landscapes such as those found on Mars.

This report details the findings of a summer research project focused on the dynamics of barchan dunes and their interaction with obstacles. The primary objective of this study was to investigate how obstacles of various sizes and shapes influence the movement, shape, and stability of barchan dunes. By simulating different scenarios in both a computational as well as experimental setting, the research intends to shed light on the behavior of these dunes.

The research was conducted using a combination of researching field observations, laboratory experiments, and numerical modeling. Field observations provided baseline data on dune morphology and movement patterns, while laboratory experiments allowed for the controlled manipulation of variables such as wind speed, sand grain size, and obstacle characteristics. Numerical models were employed to simulate dune dynamics over longer timescales and to predict the potential impacts of various environmental changes. This was combined with a study of computational fluid dynamics so that the behavior of the dunes in interaction with obstacles could be modeled more realistically.

Key questions addressed in this research include:

1. How can barchan dunes be reproduced experimentally in a lab setting?
    1. How can the experimental apparatus be designed?
    2. How can the experiment be designed and carried out?
2. How can barchan dunes and their interactions with obstacles be numerically simulated?
    1. How can the complexities of barchan dynamics be represented in a simple numerical model?
    2. How can the change in the flow around obstacles and its effect on barchans be simulated numerically?

In the following sections, we present a comprehensive overview of the methodologies employed, the results obtained, and the conclusions drawn from this summer research project on barchan dunes and their interactions with obstacles.

# II. Experiment

**Goal**: To reproduce barchan dunes on a small length scale in an experimental setting.

## II.1. Design of the experimental apparatus

The primary conditions that need to be reproduced were -

1. Unidirectional apparent wind direction above the threshold for grain entrainment.
2. Control over the wind velocity.
3. Avoidance of secondary flows that can deform the barchan.

This was required because Barchans are primarily formed due to two processes:

- **Saltation**: The entrainment of sand grains into the air by the action of wind flow - essentially flinging the sand from its initial resting place to a certain distance.
- **Avalanching**: The process by which sand that is at a resting angle that is greater than the angle of repose slides and deposits itself further downstream until the angle of repose is reached.

Additionally, as referenced in [1], the distance that is traveled by a saltated grain ($l_d$) is related to the mean density of the grain ($\rho_s$), the density of the fluid flowing over the sand bed ($\rho_f$), and the diameter of the grain ($d$) by the equation:

$$l_d = \frac{\rho_s}{\rho_f} d$$

So if we can reduce the relative density of the sand grain concerning the fluid ($\frac{\rho_s}{\rho_f}$), and use sand of a finer diameter, we can reproduce the normally huge barchans on a much smaller, centimeter-order, lengthscale. It is due to this that we take two important decisions:

- **Water would be the fluid of choice**. We could have used denser fluids, but they would be too difficult to procure and manage in the apparatus.
- The sand would be **102 micron Silicon Carbide**. It is easy to procure and there is literature on the specific cohesive effects between silicon carbide sand grains ([2]).

**An interesting feature to note here is that Barchans are essentially scale-invariant structures and occur at all length scales and timescales.** (Though there is some evidence to suggest that this might not be the case, namely - [3]).
In [1], they reproduced Barchans on a small scale in subaqueous conditions using a submerged plate that was subjected to asymmetrical vibrations such that one direction of vibration was above the threshold of sand entrainment and the other was under the threshold. This gives us strong evidence that stable Barchans can be reproduced on centimeter-order lengthscales.

### Initial designs

Several options were considered for the experimental apparatus that could reproduce these conditions. A few of them are represented below:

1. Fig. 1 — A flat table with water running over it from a reservoir elevated above it.


2. Fig. 2 — A closed chamber with a pump driven flow across it

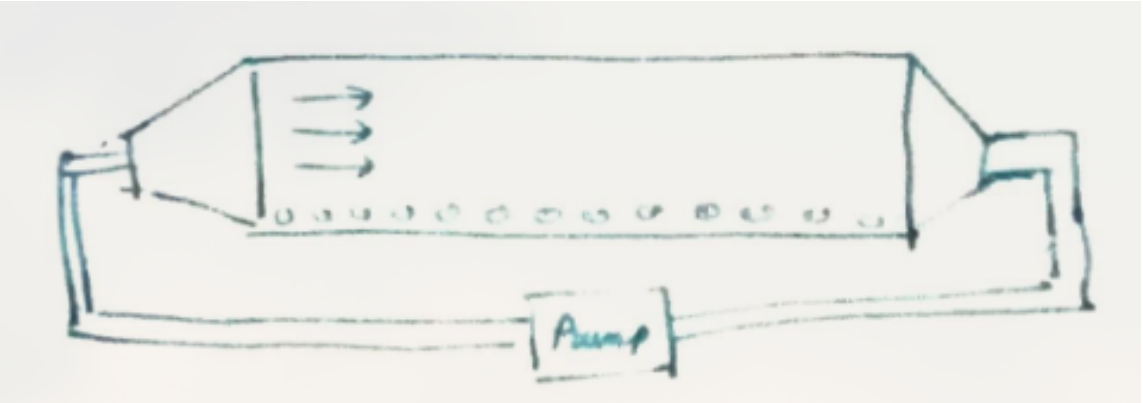


These designs were later rejected due to them being difficult to water-seal, or due to the unpredictable turbulence of the flow through them. A more elegant solution was sought that would not face such difficulties and could utilize a rheometer that was available in the lab to control the flow.

## Final design

Fig. 3 — Rough schematic of the final design for the main experimental apparatus

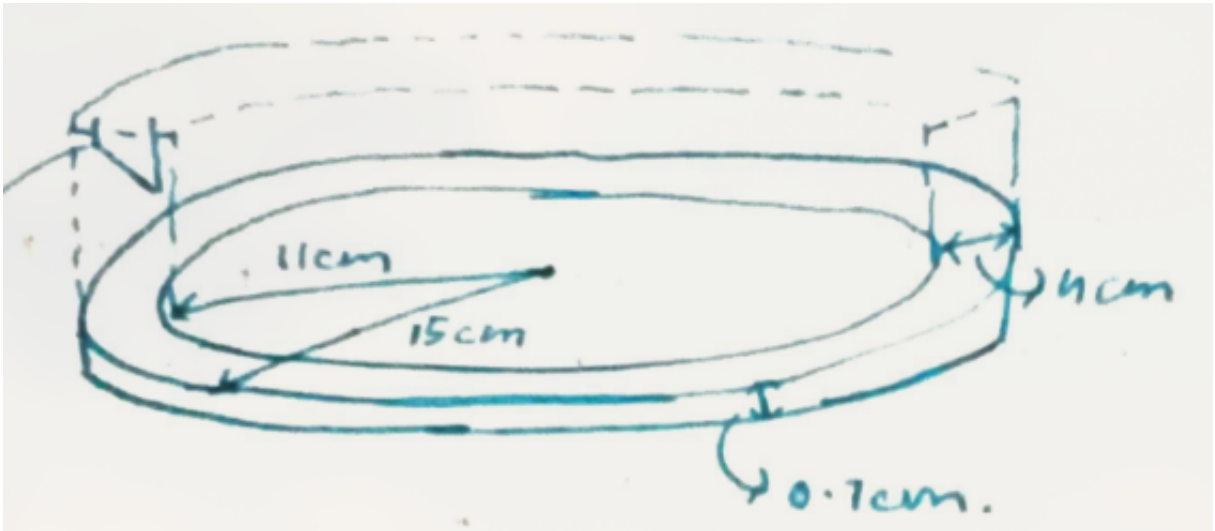

In [4], they used a circular flume that is 97cm(outer radius) and with a flume width of 9 cm, to reproduce two-dimensional Barchan dunes. Other experiments [5], have reproduced 3D Barchan dunes using pressure-driven path flow. We sought to reproduce these 3D Barchans using the flume apparatus instead of the pressure-driven flow apparatus due to the reasons outlined above.
We also chose to use 102-micron silicon carbide sand and did not use a diameter that was lower due to cohesive effects that were warned of in [1] in sand that is below 100 microns in diameter.
The experimental apparatus that we designed consists of

- a circular flume with outer radius of 15 cm and an inner radius of 11 cm with straight walls that are 8 cm high
- an angled paddle that could provide constant shear to the fluid filling the channel
- support ring and disc to ensure that the walls are perfectly straight
- attachment for the paddle to the rheometer

The channel width is 4 cm which gives us a width-to-radius ratio of 0.26, which is << 1, so we can reasonably expect an approximately local straight flow in the channel on the order of length of the Barchans. The base of the flume was made using a 0.7 cm thick acrylic plate that was laser-cut to the specific dimensions. The walls of the flume were constructed out of OHP sheets that provided transparency for imaging the channel and were rigid enough to hold the water inside the flume without warping.

Fig. 4 — Paddle design

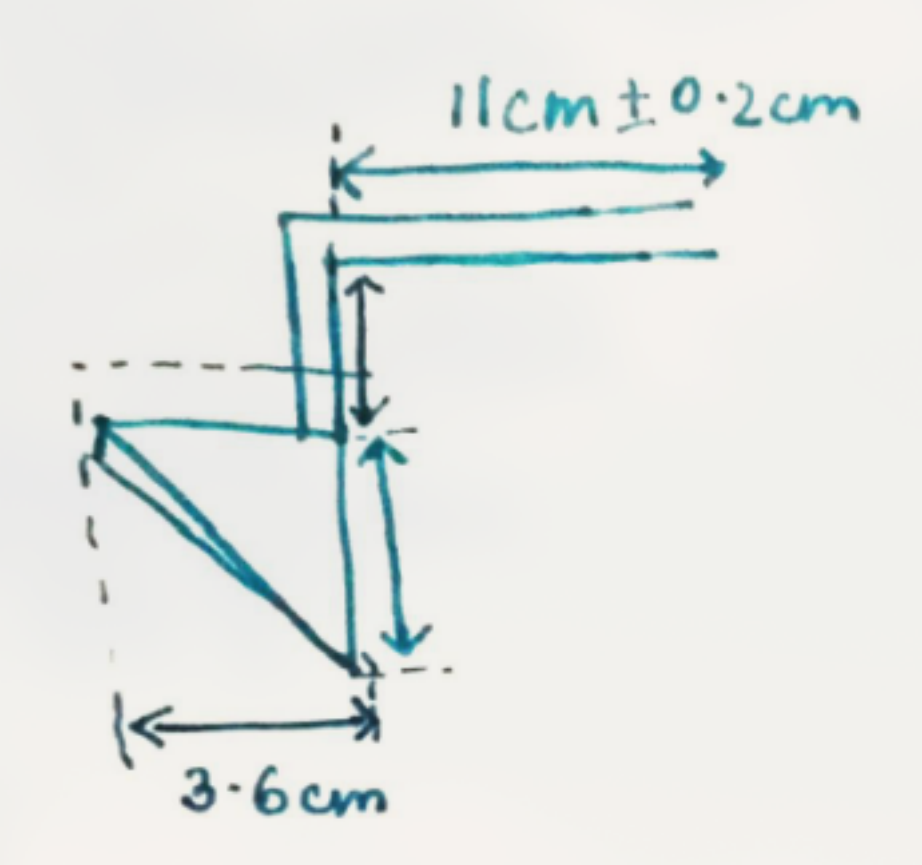

The paddle was designed with inspiration from cone-and-plate viscometers that are used to measure the rheological properties of minute samples. The angled paddle in the cone-and-plate viscometer provides a constant shear to the fluid. We sought to do the same with our paddle in order to avoid complicated secondary flow problems during the spin-up of the apparatus.
This was created by laser cutting angled (20-degree) support structures (as depicted in the figure above) and attaching a smooth strip of OHP sheet on the angled face. This prevented edge effects from sharp paddle edges in the fluid during rotation.
The paddle apparatus would be attached to the rheometer along its central axis. The rheometer would rotate the paddle apparatus at a constant angular velocity. After the spin-up period, the fluid in the flume would also be rotating at this angular velocity. The rheometer would be run in a constant shear mode which adjusts the shear rate to keep the angular velocity constant despite friction from the flume walls.
The sand would be deposited at the bottom of the flume in a conical heap and after the spin-up, it is expected that it would gradually evolve into a Barchan. All obstacles would also be similarly placed at the base of the flume channel.

## Secondary flow problem

According to [6], the Einstein tea leaves paradox poses a problem in our experimental setup. This problem can be demonstrated by the simple swirling of tea leaves to the center of a stirred cup of tea.

Fig. 5 — Illustration of the secondary flow in a stirred cup

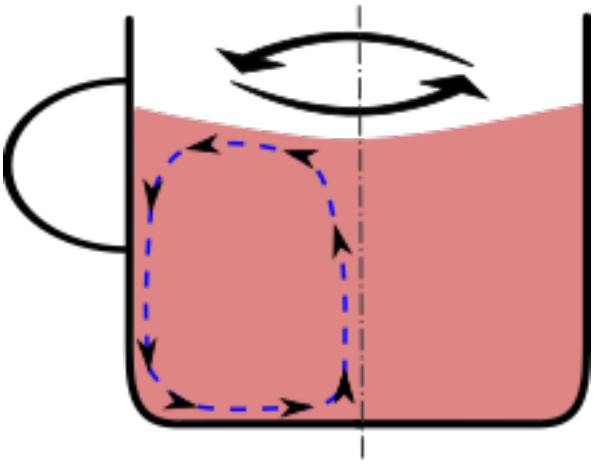

Similar to the setup of the paradox, the water in the flume is a rotating body of fluid in contact with the walls of the container that provide friction. Though the frictional effect of the outer flume surface is countered by the inner flume surface, the effect of the base plate friction is not countered by anything in the setup. This could cause a secondary flow in the inward direction, which could potentially deform the shape of the barchan (as perfect barchans are formed under unidirectional wind flow parallel to their direction of propagation). Several measures were considered to counterract this effect:

1. Non-moving lid with a sliding seal that could counterract the effect of the base plate friction
2. Filling the flume with straws to ensure that the flow is in the direction that we desire

3. Adding a counter-rotation to the base plate to counteract the effects that cause the secondary flow. (The authors of [4] do this)

Finally, in discussion with my guide, we arrived at the following conclusions regarding this problem:

- The secondary flow is not going to be of an order that will skew results in our experiment.
- The addition of lids and straws might cause other secondary flows in our system, causing more hinderances.

So we decided to forgo correcting for the secondary flow in our apparatus.

## II.2. Experiment

The experiment could not be conducted due to problems with the experimental apparatus construction, and due to a lack of time.

# III. Simulation

The simulation work was started after taking inspiration from [7] and [8], both of whose work deals with numerically simulating the behavior of sand fields under simple unidirectional wind flow, eventually obtaining barchans. This led us to [9] which was the first paper that established numerical simulations of barchans.

## III.1. Werner Cellular Automata model

Fig. 6 — Werner cellular automata model

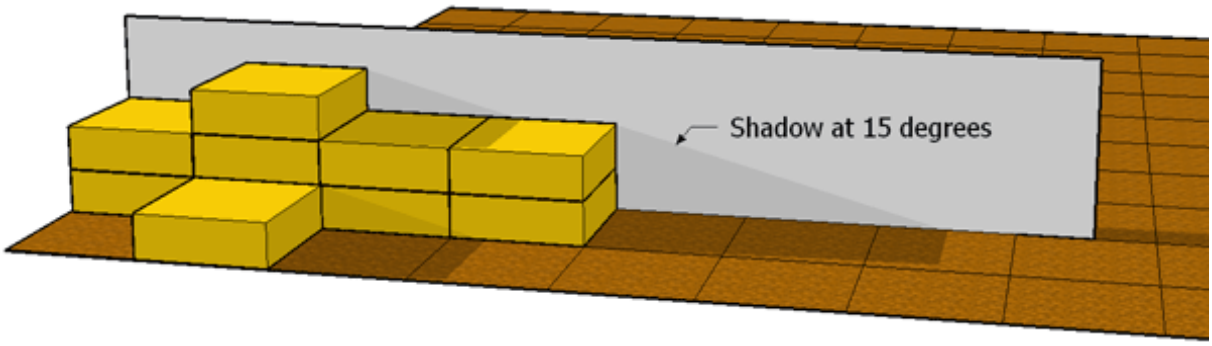


The model put forward by [9] is essentially a simple cellular automata simulation with the following rules specified:

1. The sand field is comprised of cells $(x, y)$, each of which has an assigned height of sand $(h_{x,y})$.
2. The sand casts a shadow in the downstream (concerning the wind flow) direction, decided by some fixed angle, approximating the extent of a recirculation cell downwind of a slipface of a dune.
3. Cells are said to be in the shadow if it is the shadow of some cell that is upwind of it.
4. Sand transport is carried out by selecting a cell randomly from the grid and carrying out two processes on it:
    1. **Saltation**: A slab of sand (some fixed height of sand) is picked up from the selected cell and deposited in another cell. If this second cell is in the shadow, then the sand is deposited there with a probability of 1. If it is not in the shadow but is covered by sand, then it is deposited with a probability of 0.6, and if the cell is not in the shadow and is bare, then it is deposited with a probability of 0.2. If the sand is not deposited, then the process repeats until the sand has been deposited.
    2. **Avalanching**: The cell where the sand was deposited is checked to see whether any of the **8** (Moore neighborhood, not the von Neumann neighborhood) immediately neighboring cells have a sand height such that an avalanche of sand can occur from the deposit cell to that cell. If such a cell is found, a fixed height of sand is taken from the deposited cell and put on the neighbor cell, simulating a slip of sand. This process is repeated on that neighboring cell until a state is reached where no avalanche can occur.

In addition to this, it is to be noted that the model allows for no erosion in the shadow, i.e. there is no saltation for the sand that is present in the shadow.

This scheme was implemented in Python and C++, and the **resulting dunes had the characteristic barchan shape**.

Fig. 7 — Barchan dune shape formed by the initial simulation model

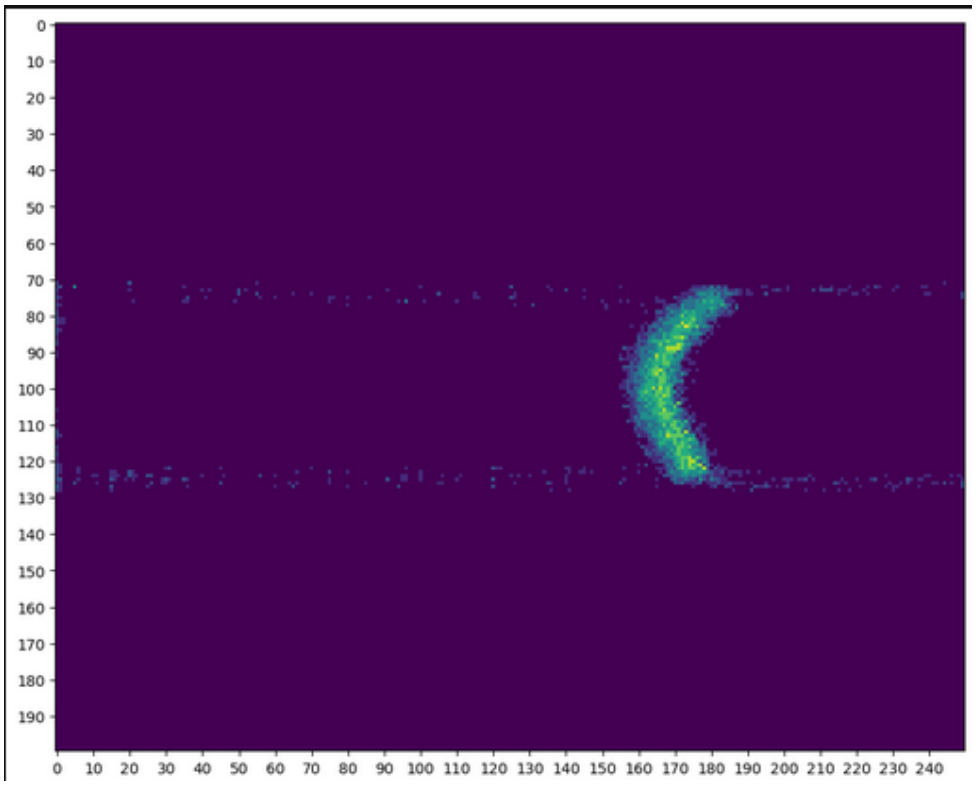


We measured the length and width of the simulated barchans (which evolved from initial conical sand piles of different sizes) and fitted them with a straight-line equation ($y = Ax + B$). We expected a reasonably good fit, in line with the results from [1].

Fig. 8 — Fit, $A = 0.8306 \pm 0.0681$, $B = -7.4592 \pm 4.7169$

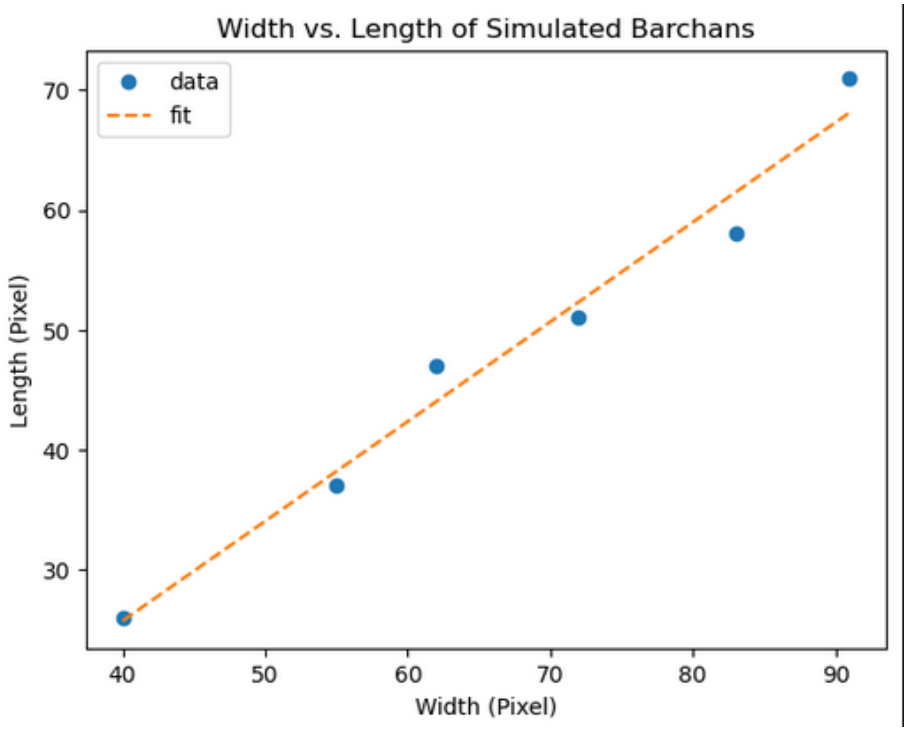

Thus, we can conclude that the results obtained do agree with the expected results. Comparison with data from field studies is left to be done.

## III.2. Computational Fluid dynamics

To capture the behavior of barchans interacting with obstacles of different shapes and sizes, it was necessary to model the flow of fluid around these obstacles. This was done in two ways:

1. Solving the discretized Navier-Stokes equations for a stable pressure-driven flow across an obstacle.
2. Using the Lattice Boltzmann method to numerically simulate unstable turbulent flow around an obstacle.

### Pressure driven potential flow

In some cases, fluids can be modeled using a scalar potential function instead of a velocity field, which are related through:

$$\vec{v} = \vec{\nabla}\varphi$$

In 2 dimensions, the Laplace equation for the potential is written as follows:

$$\frac{\partial^2\varphi}{\partial x^2} + \frac{\partial^2\varphi}{\partial y^2} = 0$$

This problem will be solved on a grid that features an airfoil-like obstacle region. This can be done by defining boundary conditions on the outer boundary $\Gamma_0$ (flow undisturbed here) and the inner boundary $\Gamma_i$ (the flow does not penetrate the obstacle region). This is written as:

$$\vec{v}(x) \cdot \vec{n}(x) = \vec{v_0} \cdot \vec{n}(x) \forall x \in \Gamma_0$$

Where $\vec{v_0}$ is the initial velocity of the fluid.

$$\vec{v}(x) \cdot \vec{n}(x) = 0 \forall x \in \Gamma_i$$

These equations are then discretized using naive finite differences and then solved on the grid.

Fig. 9 — Potential and velocity field with a cylindrical obstacle

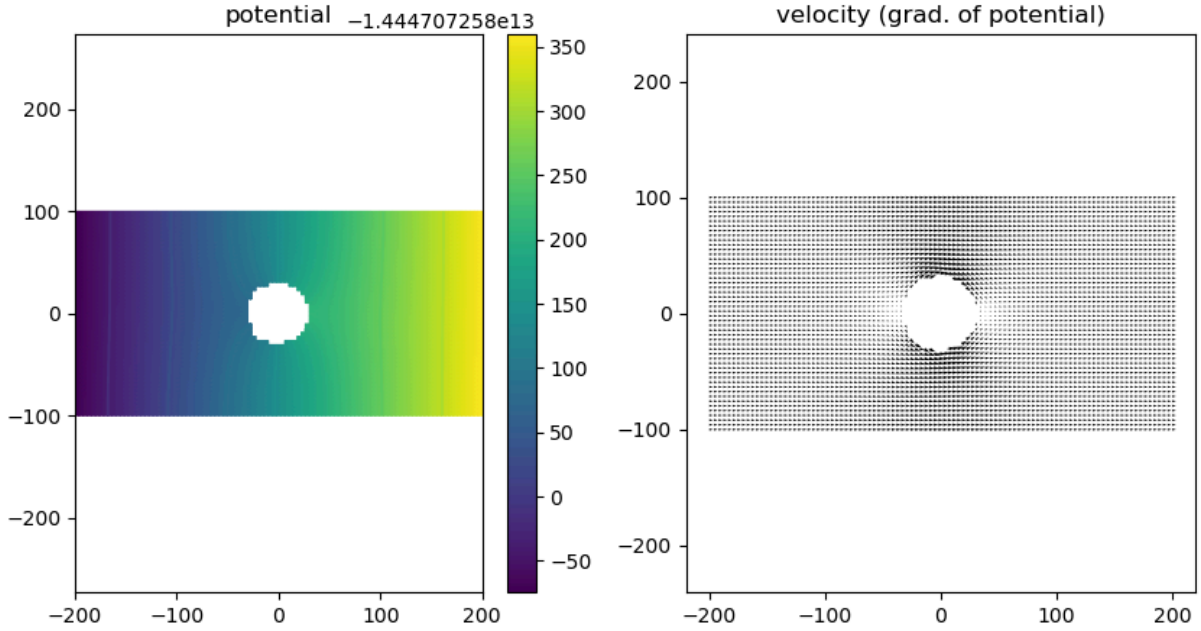

Fig. 10 — Streamline plot of the fluid flow around a cylindrical obstacle

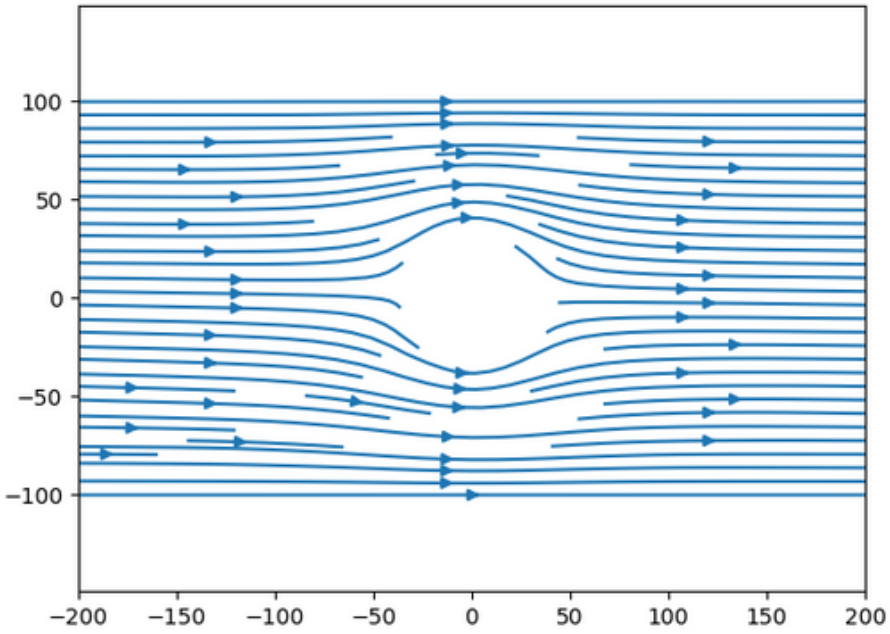


This CFD solver was integrated into the Werner model cellular automata by altering the code such that the direction and distance of the saltation of a particular grain were determined by the velocity vector at that grid location.

Among the behaviors that were visualized using this simulation, the most notable was the **calving** of the barchan dune into two dunes before colliding with the obstacle. There was also a corresponding elongation and asymmetry observed in the original barchan.

Work on the dynamics of sand collision with the obstacle is still underway, but it was also observed that sand was captured in the wake of the obstacle. The amount of sand captured in the wake and upwind of the obstacle, and the reformation of barchans downwind of the obstacle (if any) may be interesting variables to study - as information regarding these quantities is essential to predicting the behavior of migrating barchans that encroach on infrastructure.

Fig. 11 — Calving event before collision (Cylindrical obstacle is not visible in this image)

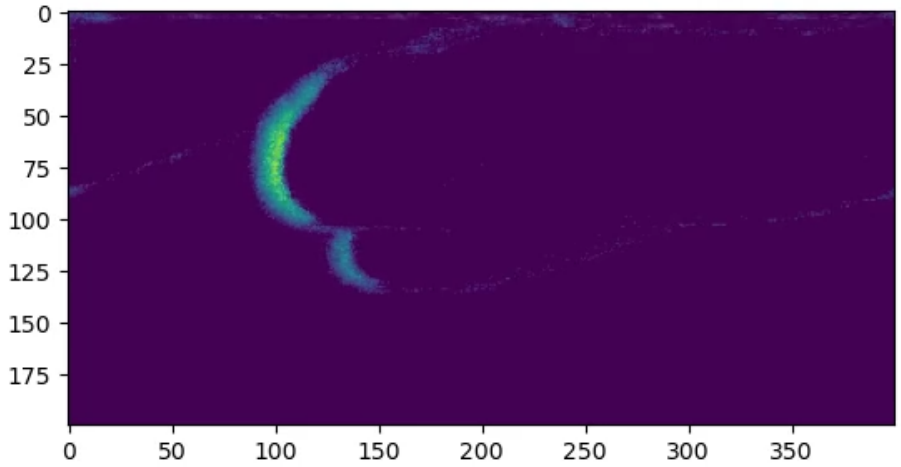


As of now, this model can only be treated as a qualitative representation of the dynamics of a barchan dune interacting with the obstacles.

## Lattice Boltzmann method

The Lattice-Boltzmann algorithm provides us with a method for doing computational fluid dynamics that does not involve discretizing and solving the Navier-Stokes equations. Instead of doing that, we think of the fluid as a collection of molecules that exist on a grid. For each generation of the simulation, we imagine that these particles move to adjacent cells on the grid and that they collide with other particles. The macroscopic properties of the fluid in each cell of the lattice (density, velocity, etc) can then be computed from the particles that it contains.

Suppose that the fluid is an ideal gas, and suppose that it has a macroscopic velocity $\vec{u}$ and is in thermal equilibrium at a temperature $T$. Then, the molecules will have thermal velocities $\vec{v}$ that are distributed according to the Boltzmann distribution. For a 2D gas, the distribution is:

$$D(\vec{v}) = \frac{m}{2\pi kT} \exp\left(\frac{-m\ |\vec{v}|^2}{2kT}\right)$$

Where $m$ is the mass of each molecule, and $k$ is the Boltzmann constant.

In the LB Method, we discretize both space and time so that only certain velocity vectors are allowed. In this case, we use the **D2Q9** lattice, in which there are only two dimensions and 9 allowed displacement vectors - perfectly suited for the 2D cellular automata model that we are working with.

Now, we attach probabilities to these nine velocity vectors, to model the continuous Boltzmann distribution as accurately as possible. For a fluid at rest (i.e. $\vec{u} = 0$), the previous equation gives the most and least probable velocities with the following probabilities or weigths $w_i$ for each of the nine directions:

Fig. 12 — Directions in which the molecules can move in

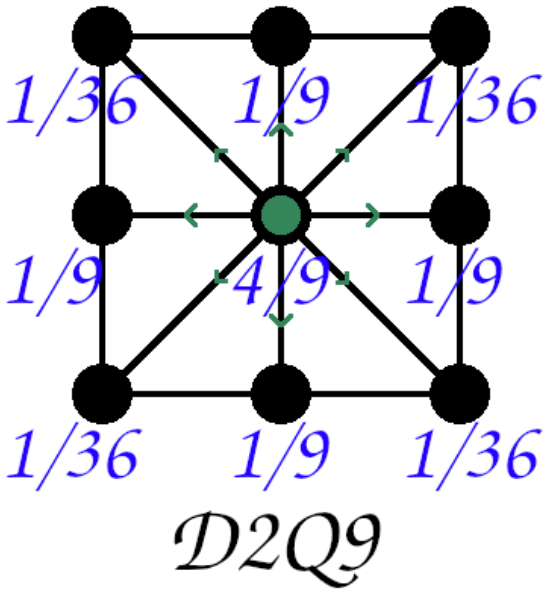


The steps of the algorithm are:

1. **Streaming**: All the particle number densities move into the adjacent/diagonal lattice cells.
2. **Bouncing**: All the particle number densities that have streamed into a cell containing a barrier are reflected back to the direction that they came from.

3. **Collisions**: From the new set of number densities contained within each cell, we compute what densities would be if the molecules in that cell were in thermal equilibrium. Then, we proceed to update all the densities in the cell toward this equilibrium state.

We can describe the microscopic particles that make up the fluid using the distribution function $f(\vec{x}, \vec{v})$ which describes the phase space density of fluids at location $\vec{x}$ traveling with velocity $\vec{v}$

The streaming and the colliding behavior can be captured by the BGK approximation (Bhatnagar-Gross-Krook):

$\left(\frac{\partial}{\partial t} + \vec{v} \cdot \vec{\nabla}\right) f = -\frac{f - f^{eq}}{\tau}$

Where the left-hand side represents streaming and the right-hand side approximates collisions (with time scale $\tau$). In this approximation, the distribution function $f$ tends towards some equilibrium state $f^{eq}$ as a result of the collisions and streaming.

This equation may be discretized onto the lattice. Moments of the discrete distribution function can be taken to recover the fluid variables at each lattice site.

This method was implemented in Python, and a test case scenario was run with a cylindrical obstacle in a periodic box with rightward moving fluid. It was expected that as the simulation evolved, turbulence would develop in the wake of the cylinder, leading to the well-known pattern of the **Karman vortex street**.

Fig. 13 — Von Karman vortex street generated by the LBM simulation

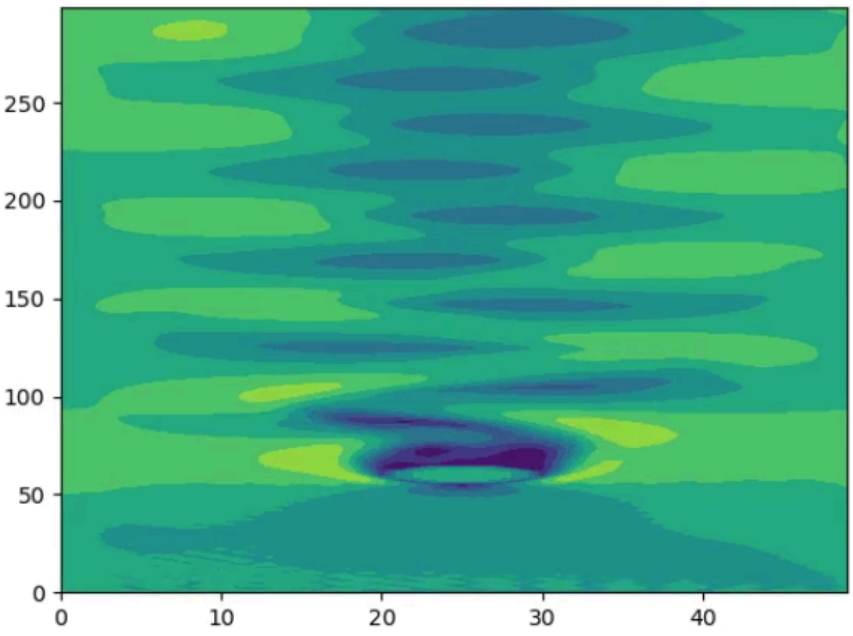


Integration of this model with the cellular automata is still underway, and we expect to see much more complex behavior from the barchans interacting with obstacles under the influence of this model. The turbulence that is being modeled might be the cause of the most interesting behavior, as it may prevent the formation of barchans or alter their shape in the wake of the obstacle.

### Global avalanching rules

The avalanching rule that was specified in the original model by Werner ([9]), was seen to be too simplistic for real sand dunes due to the following reasons:

1. Sand does not always immediately avalanche when the angle of repose is reached or exceeded.
2. Avalanches are a global phenomenon, i.e. a small avalanche or a deposition of sand can be enough to trigger a much bigger avalanche, which in turn can trigger even bigger avalanches. This behavior is not captured by the previous model.

To capture this behavior, we came up with a new set of rules for avalanching:

1. Initially, every point on the grid of sand will be evaluated to see whether the angle or repose is exceeded concerning any of the 8 immediate neighbors. If it is exceeded, then the grid point is assigned a **probability of avalanching** that is *proportional to the steepness of the highest slope with its neighbors*. Let us call this initial probability at the grid location $(i, j)$ as $p^0_{i,j}$.
2. When a slab of sand is deposited, it is counted as a perturbation. The probability of avalanching in the neighborhood of the deposition spot is increased by a value that is proportional to $\frac{1}{d^2}$, where $d$ is the linear distance from the deposition spot and the cell being updated (This is done under the assumption that the energy from the perturbation dissipates in a spherically symmetric fashion). If $p^0_{i,j} + \beta\frac{1}{d^2} > 1$, $p_{new} = 1$, otherwise $p_{new} = p^0_{i,j} + \beta\frac{1}{d^2}$, where $\beta$ is some constant that measures the cooperativity of the avalanche processes.
3. A matrix of random numbers $(x_{i,j})$ is generated with $x_{i,j} \in [0, 1]$. If $x_{i,j} > p_{i,j}$, an avalanche is triggered there. A slab of sand is moved from that cell to the cell which it has the steepest angle with. The probability of avalanching at this position is set to zero. In all the positions where this condition is not satisfied, avalanching does not occur, and the probabilities remain the same.
4. This avalanche, in turn, is also counted as a perturbation. Similar to the perturbation from the deposition of sand, the avalanching probabilities in the neighborhood of the avalanching cell are increased proportionally to $\frac{1}{d^2}$.
5. The matrix of random numbers is generated again, and the process for initiating the avalanches is repeated. This continues until either a set upper limit of propagated avalanches (for computational cost reasons, this had to be implemented) is reached, or there are no more avalanches that have been initiated.

This model was also incorporated into the code, and the results seemed to show a greater realism in the case of sand avalanches as compared to the previous model. This manifested itself in smoother slopes of barchans, and more realistic and spread out slipface.

## IV. Additional work

Some additional work was done regarding the barchans that do not fit into the categories mentioned above.

## IV.1. Self-Organized Criticality (SOC)

First introduced by [10], the concept of Self-Organized Criticality has pervaded the study of many systems. Particularly interesting among these systems, for our study, is the fact that Per Bak and his colleagues created a model for a sand pile - where the avalanches on the slope of the pile followed SOC behavior. It was shown by Sidney R. Nagel [11] that sand piles do not demonstrate SOC behavior in real life.

When a pile of sand is exactly at its angle or repose, it will suffer a lot of little landslides. A few of these landslides will become big. The theory of critical phenomena suggests that in this situation, the probability that a landslide grows to size $L$ should satisfy a power law, i.e. it should be proportional to $\frac{1}{L^c}$ for some number $c$ called the critical exponent. This type of behavior is seen in many situations where the system is on the brink of some drastic change, i.e. some critical point.

When the system is not at a critical point, we observe exponential laws where the probability of a disturbance of size L is proportional to $\exp\left(-\frac{L}{L_0}\right)$ where $L_0$ is a fixed length scale. The direct implication of this is that systems that are at a critical point are self-similar - i.e. it has no specific length scale.

The idea of self-organized criticality introduced by [10] says that some physical systems (like sand piles and dunes) seem to spontaneously bring themselves towards critical points without any need for us to tune their parameters to special values.

The question of whether our new global avalanching model (explained previously) is any better concerning following SOC (or not following SOC) was of interest to us.

To test how the model performed in comparison to the older model, we sought to test the power laws that avalanches in SOC systems follow.

Fig. 14 — SOC Power law graph for the Werner avalanche rule

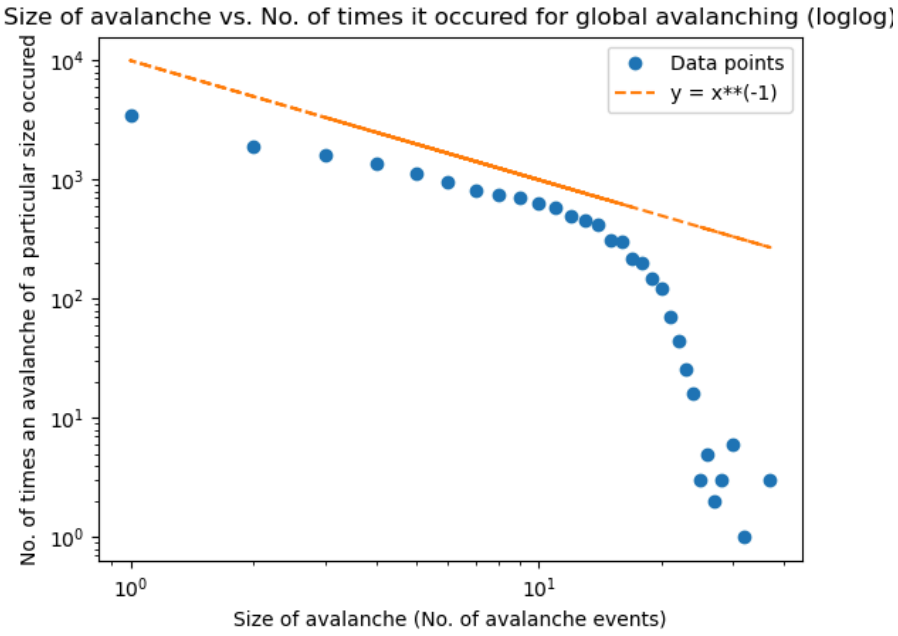

Fig. 15 — SOC Power law graph for new global avalanche rule

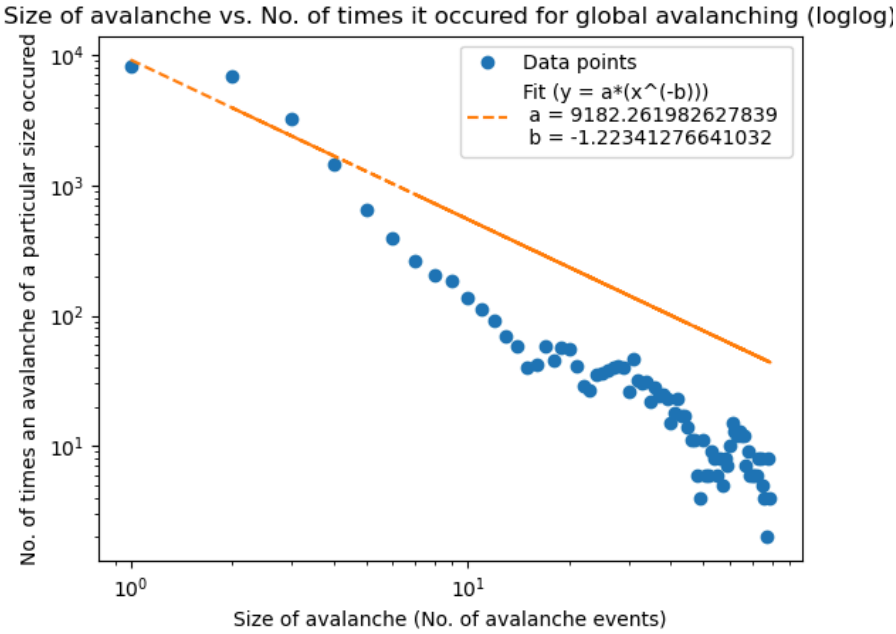


As it can be seen, the older rule follows the power law quite closely up until a certain cutoff size. The newer rule, on the other hand, does not follow the SOC power law as closely and seems to have a noticeable deviation after a certain point.

We hypothesize that this is because the newer rule mimics the nature of sand avalanches more closely, i.e. there is a finite probability that an avalanche will not happen even if the angle of slope is greater than the angle of repose of the sand.

For further work on this avenue, we need to compare the results from the new rule to the results that were obtained by [11].

## IV.2. Equation of surface of the barchan dune

Fig. 16 — Schematic diagram of a barchan dune

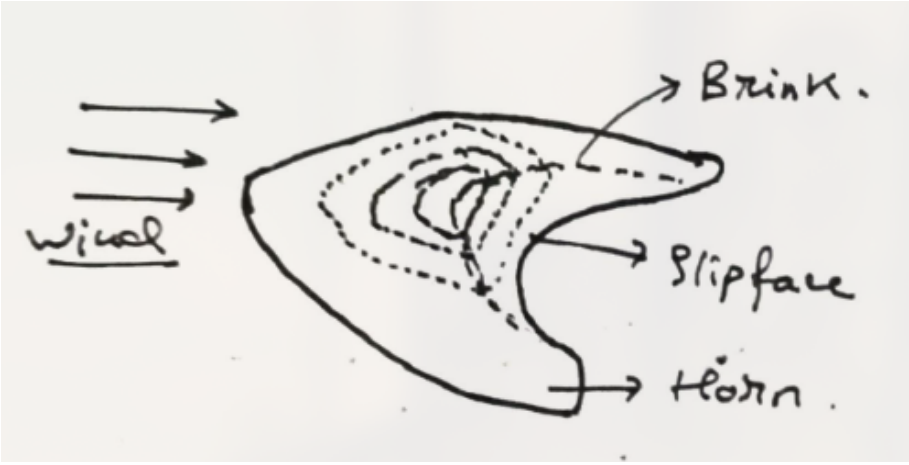


Inspired by the work of [12], we sought to understand why Barchan dunes are such general structures - they form wherever there is scarce granular matter present with a fluid flowing over it above a certain threshold shear rate.

We hypothesize that some variable is being optimized in the case of the barchan, i.e. the barchan shape is optimizing some quantity. We think that the barchan is optimizing the trapping efficiency (that fraction of the incoming sand flux on the barchan that is trapped in the separation bubble) because the barchan is a self-sustaining shape that migrates while having little to no change in its size and shape under a wide variety of wind velocities. To confirm this, the first step would be to understand the shape of the barchan and to quantify it precisely so that models could be made of it and tested further.

Since the barchan has an asymmetric shape in a longitudinal (along the wind) cross-section, we start with an asymmetric sinusoid $y = a\sin(x - b\sin(x))$.

Next, we know from [13] that the windward and leeward feet of the barchan approximate a parabolic profile quite closely. Integrating this fact, along with a few other tweaks, we arrive at the equation:

$$z = -f(ax^2 + bx + c)\sin^2(y - x^2 - d\sin^2(y - x^2))$$

Fig. 17 — Angled view of the graph of the equation

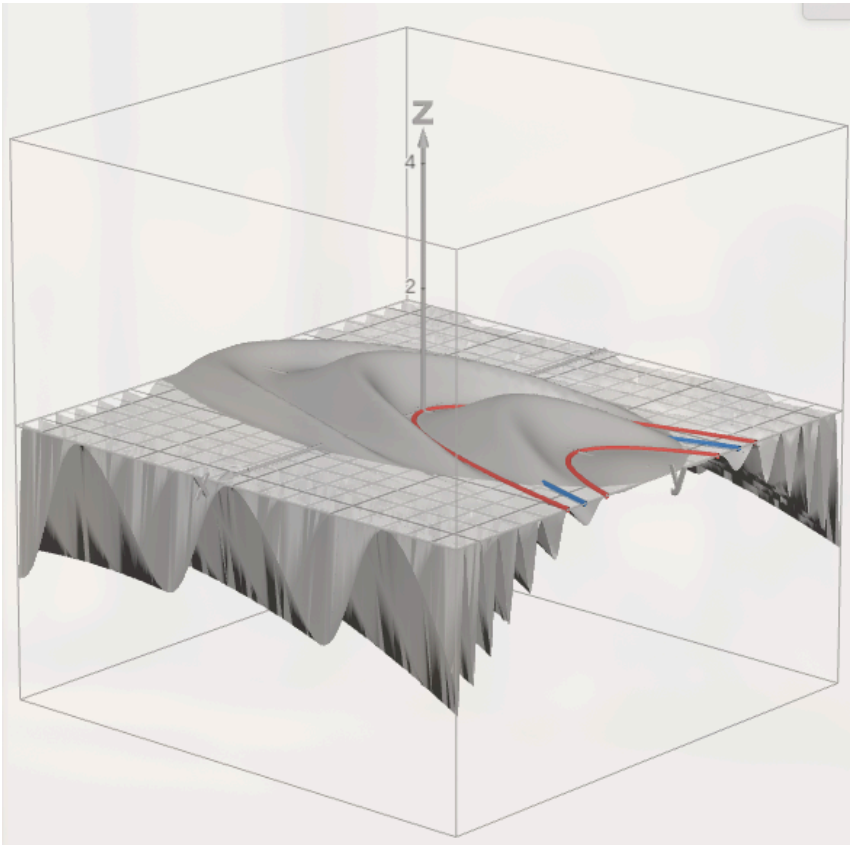

Fig. 18 — Top view of the graph of the equation

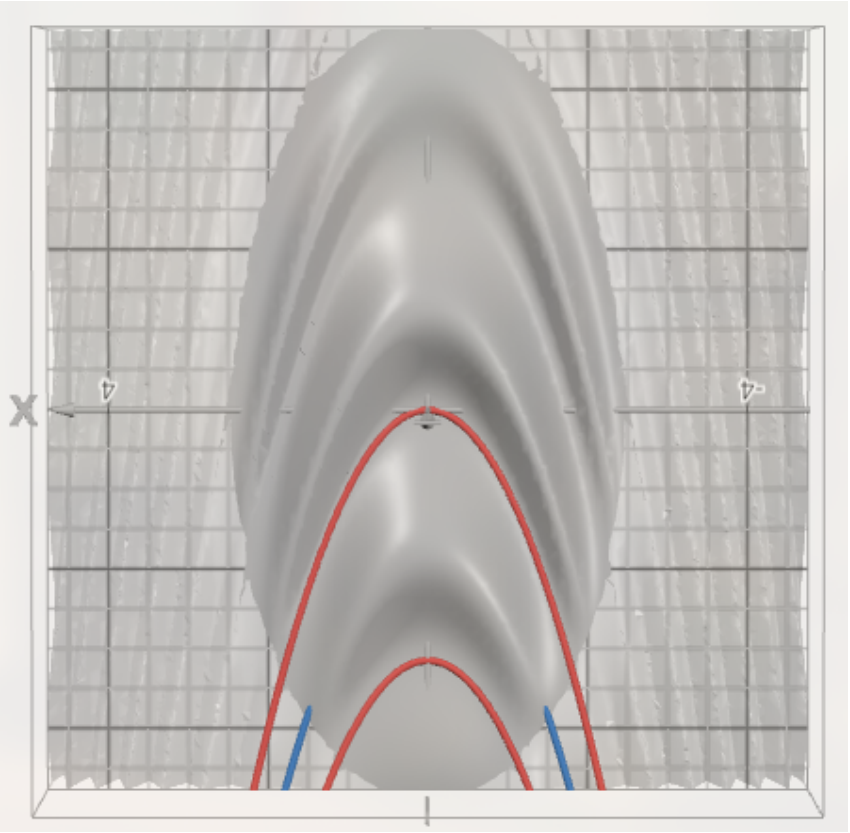

The graphs look quite similar to barchans qualitatively, but we can not say for sure that this is the equation of the surface of the barchans until we fit the equation with field data. This could not be done due to the lack of time, and difficulty in finding tabulated field measurements that could be used for this purpose.

# Bibliography

[1] P. Hersen, S. Douady, et B. Andreotti, « Relevant Length Scale of Barchan Dunes », *Physical Review Letters*, vol. 89, n° 26, p. 264301-264302, déc. 2002, doi: 10.1103/PhysRevLett.89.264301.

[2] N. Preud'homme, E. Opsomer, F. Francqui, A. Neveu, et G. Lumay, « EFFECT OF COHESIVE FORCES ON GRANULAR FLOWS IN ROTATING DRUM: LINKING EXPERIMENTS AND SIMULATIONS ».

[3] K. Kroy et X. Guo, « Comment on "Relevant Length Scale of Barchan Dunes" », *Physical Review Letters*, vol. 93, n° 3, p. 39401-39402, juill. 2004, doi: 10.1103/PhysRevLett.93.039401.

[4] K. A. Bacik, P. Canizares, C.-c. P. Caulfield, M. J. Williams, et N. M. Vriend, « Dynamics of migrating sand dunes interacting with obstacles », *Physical Review Fluids*, vol. 6, n° 10, p. 104308-104309, oct. 2021, doi: 10.1103/PhysRevFluids.6.104308.

[5] C. A. Alvarez et E. M. Franklin, « Birth of a subaqueous barchan dune », *Physical Review E*, vol. 96, n° 6, p. 62906-62907, déc. 2017, doi: 10.1103/PhysRevE.96.062906.

[6] K. Kolesnik, D. Q. L. Pham, J. Fong, et D. J. Collins, « Thomson–Einstein's Tea Leaf Paradox Revisited: Aggregation in Rings », *Micromachines*, vol. 14, nº 11, p. 2024-2025, nov. 2023, doi: 10.3390/mi14112024.

[7] A. Katsuki, M. Kikuchi, et N. Endo, « Emergence of a Barchan Belt in a Unidirectional Flow: Experiment and Numerical Simulation », *Journal of the Physical Society of Japan*, vol. 74, nº 3, p. 878-881, mars 2005, doi: 10.1143/JPSJ.74.878.

[8] A. Katsuki, M. Kikuchi, H. Nishimori, N. Endo, et K. Taniguchi, « Cellular model for sand dunes with saltation, avalanche and strong erosion: collisional simulation of barchans », *Earth Surface Processes and Landforms*, vol. 36, nº 3, p. 372-382, mars 2011, doi: 10.1002/esp.2049.

[9] B. T. Werner, « Eolian dunes: Computer simulations and attractor interpretation », *Geology*, vol. 23, nº 12, p. 1107-1110, déc. 1995, doi: 10.1130/0091-7613(1995)023<1107:EDCSAA>2.3.CO;2.

[10] P. Bak, C. Tang, et K. Wiesenfeld, « Self-organized criticality: An explanation of the 1/f noise », *Physical Review Letters*, vol. 59, nº 4, p. 381-384, juill. 1987, doi: 10.1103/PhysRevLett.59.381.

[11] S. R. Nagel, « Instabilities in a sandpile », *Reviews of Modern Physics*, vol. 64, nº 1, p. 321-325, janv. 1992, doi: 10.1103/RevModPhys.64.321.

[12] « Geometry and dynamics link form, function, and evolution of finch beaks ». Consulté le: 18 juin 2024. [En ligne]. Disponible sur: https://www.pnas.org/doi/10.1073/pnas.2105957118

[13] G. Sauermann, P. Rognon, A. Poliakov, et H. Herrmann, « The shape of the barchan dunes of Southern Morocco », *Geomorphology*, vol. 36, nº 1–2, p. 47-62, déc. 2000, doi: 10.1016/S0169-555X(00)00047-7.